Differential Elastic Scattering of 15.2-MeV Neutrons by Ta, Bi, Th, and U*

CECIL I. HUDSON, JR.,† W. SCOTT WALKER,‡ AND S. BERKO§
University of Virginia, Charlottesville, Virginia
(Received May 17, 1962)

Angular distributions of 15.2-MeV neutrons elastically scattered by Ta, Bi, Th, and U have been measured using an associated particle time of flight system with an energy resolution of 1.8 MeV at 15.2 MeV (defined as the energy loss for which neutrons are detected with 50% efficiency relative to elastically scattered neutrons) and an angular resolution of ±2°. The data were corrected for multiple scattering and attenuation by Monte Carlo methods, and the results are compared with the theoretical optical model predictions of Bjorklund and Fernbach for spherical nuclei. For Ta, Th, and U, the diffraction pattern appears damped in the backward angles, an effect attributable to the large deformations present in these nuclei.

I. INTRODUCTION

THERE have been many measurements of elastic differential cross sections of 14- to 15-MeV neutrons scattered from nuclei having a wide range of atomic weights.[1] These measurements have not included any detailed studies of scattering by deformed nuclei, and the question arises as to whether nuclear deformation produces observable effects at these energies. The angular distribution of neutrons scattered from deformed nuclei can generally be expected to have less pronounced maxima and minima than in the case where no deformation is present. Such an effect appears in high-energy electron scattering from deformed nuclei.[2] In the case of 7-MeV neutrons scattered from Al and Ta, both deformed nuclei, the differential cross section differs significantly from that predicted by the optical model calculations of Bjorklund and Fernbach.[3] A similar deviation was observed for Al at a neutron energy of 14.6 MeV,[4] but one might not expect the optical model to describe the scattering correctly for a nucleus as light as Al. Schey[5] was able to obtain better agreement with the experimental results for Ta at 7 MeV by including a deformation term as a perturbation in the potential used by Bjorklund and Fernbach; but, due to the lack of experimental data, he did not attempt to extend his computations to other nuclei or energies.

The purpose of this experiment is to see if there is any significant disagreement between the experimental results and the theoretical predictions of Bjorklund and Fernbach in the case of 15.2-MeV neutrons scattered elastically by Ta, Th, and U-nuclei having large deformations. Bi, a spherical nucleus, is included for comparison and as a standard, since it has been studied by several authors. Coon *et al.*[6] have presented preliminary data on U, and Cross and Jarvis[1] have published measurements on Ta, but these data were taken mainly for forward angles. The following paragraphs describe the experimental method, the data reduction technique, and present the corrected data.

II. EXPERIMENTAL METHOD

A. Apparatus

The University of Virginia 1-MeV Van de Graaff accelerator was used to provide a beam of 320-keV deuterons which bombarded a thin (250 μg/cm^2) tritium-zirconium target. The (n,a) associated-particle method was used to provide an "electronically collimated" beam of 15.2-MeV neutrons, and to provide a "start" signal for a time-to-pulse-height converter that was used to perform time-of-flight analysis on the scattered neutrons. This apparatus is a completely redesigned and improved version of the apparatus described in reference 7.

Figure 1 is a schematic drawing of the scattering arrangement. The neutron detector was a cylinder of

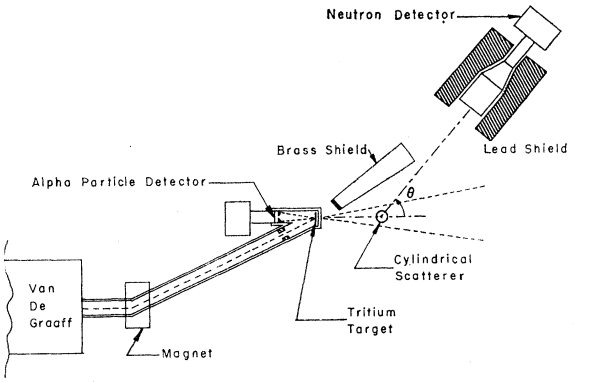

FIG. 1. Schematic drawing of experimental arrangement.

* Jointly supported by the U. S. Atomic Energy Commission and the U. S. Army Research Office.
† Now at the University of California Lawrence Radiation Laboratory, Livermore, California.
‡ Now at Hughes Aircraft Company, Culver City, California.
§ Now at Brandeis University, Waltham, Massachusetts.
[1] See list of references in W. G. Cross and R. G. Jarvis, Nuclear Phys. **15**, 155 (1960).
[2] B. Hahn and R. Hofstadter, Phys. Rev. **98**, 278 (1955).
[3] F. Bjorklund and S. Fernbach, Phys. Rev. **109**, 1295 (1958); also University of California Radiation Laboratory Report UCRL-4926-*T*, 1957 (unpublished).
[4] J. D. Anderson, C. C. Gardner, J. W. McClure, M. P. Nakada, and C. Wong, Phys. Rev. **115**, 1010 (1959).
[5] H. M. Schey, Phys. Rev. **113**, 900 (1959); also B. Margolis, Part I. C. of *Proceedings of the International Conference on the Nuclear Optical Model, Florida State University Studies, No. 32* (The Florida State University Press, Tallahassee, 1959).
[6] J. H. Coon, R. W. Davis, H. E. Felthauser, and D. B. Nicodemus, Phys. Rev. **111**, 250 (1958).
[7] S. Berko, W. D. Whitehead, and B. C. Groseclose, Nuclear Phys. **6**, 201 (1958).

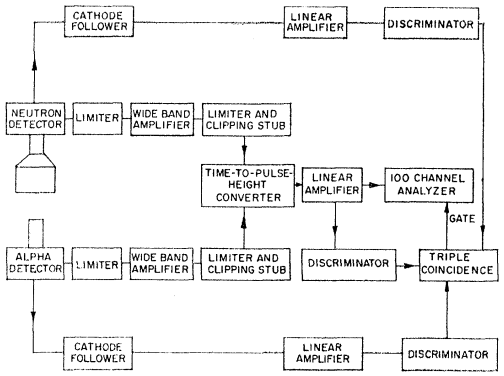

FIG. 2. Block diagram of electronics

NE 102 plastic scintillator (a product of Nuclear Enterprises, Ltd.) 13 cm in diameter and 15 cm long, coupled to an RCA 6342-A photomultiplier tube by a 10-cm conical light pipe. For the 179-cm flight path, the neutron detector subtended an angle of 4° from the scatterer. The alpha detector was a 2-mil sheet of NE 102 scintillator cemented to the face of an RCA 6342-A photomultiplier tube which also served to seal the vacuum of the tritium target assembly. A 1-cm×2-cm rectangular Al collimator was used in front of the alpha detector to insure that the alpha beam, and therefore the associated neutron beam, had a rectangular profile. The angle between the center of the deuteron beam and the center of the detected alpha beam was 145°.

Approximately half a ton of lead was used around the neutron detector to shield against background gamma rays and room-scattered neutrons. In addition, a brass or iron shadow bar was used to attenuate the direct neutrons from the source.

The scatterers were 1-in.-diam by 2-in.-long cylinders (except U which was $1\frac{1}{2}$ in. long) and were suspended by a thin wire. All scatterers had natural isotopic abundancies. The distance from the source to the scatterer was 30.1 cm.

Figure 2 is a block diagram of the electronic circuitry. The signals from the alpha-particle detector and the neutron detector were treated identically, and measured delay cables were used for all fast pulses. The phototube anode pulses were limited at the preamplifiers and were fed after amplification by Hewlett–Packard 460B distributed amplifiers to a Green and Bell[8] type time-to-pulse-height converter. The converter consisted of two pentode limiters with shorting stubs at their output feeding directly the two grids of a biased 6BN6 tube. The output of the converter was amplified and analyzed by a 100-channel Penco pulse-height analyzer gated by a triple coincidence between three slow side channels, as shown in Fig. 2. Integral discrimination was used on all three channels. The bias for the neutron detector was set sufficiently high to reject all signals due to neutrons from the d-D reaction, a major source of background from the accelerator.

The counting rate of a neutron monitor was used as a time base. The monitor was a rectangular plastic scintillator on an RCA 6342 photomultiplier tube. It was placed 1 m from the neutron target and at an angle of 90° with respect to the "electronically collimated" neutron beam. It was biased to reject all pulses due to neutrons of energies less than 5 MeV.

B. Calibration

The time-to-pulse-height converter was calibrated by varying the relative length of the delay cables between the alpha and neutron detectors and the converter, with the scatterer removed, and the neutron detector in the "beam." The position of the peak of the time-of-flight spectrum was recorded as a function of delay. This curve agreed with that obtained by varying the flight path from source to detector. The full width (at half maximum) of the time-of-flight curve was 3 nsec; the largest contribution to this width came from the time required for a neutron to traverse the length of the large detector. The same time-to-pulse-height converter produced a 0.6-nsec width when used with small scintillators on the coincident gammas from Co^{60}.

With the 179-cm flight path used in this experiment, and for 15.2-MeV neutrons, the time resolution of 3 nsec corresponds to an energy resolution of 2.5 MeV. In the actual data reduction, an integral number of channels of the time-of-flight spectrum were used as the "elastic scattering peak," corresponding to a spread in flight time of slightly more than 3 nsec. Figure 3 gives the relative efficiency for detection of neutrons of energy E for the time-of-flight system used in this experiment. If the energy resolution is defined as the energy loss for which neutrons are detected with 50% efficiency relative to elastically scattered neutrons, the system has an energy resolution of 1.8 MeV.

C. Method of Taking Data

The center of the beam was determined by pivoting the neutron detector about the source and measuring the neutron-alpha delayed coincidence rate as a function of the position of the detector. The neutron "beam" profile was also checked by using a smaller detector to insure a constant flux over the area of the scatterer.

The neutron detector was moved to the center of the beam (0°) and a time-of-flight spectrum was recorded for a given number of monitor counts, with the scatterer removed. The scatterer was then placed in the beam, the neutron detector rotated to an angle θ about the center of the scatterer, and the time-of-flight spectrum of the scattered neutrons was recorded for a given number of monitor counts. The same measurement with the scatterer removed gave the background. The channels corresponding to the elastic scattering peak were determined from the zero-degree spectrum (since energy loss

[8] R. E. Green and R. E. Bell, Nuclear Instr. 3, 127 (1958).

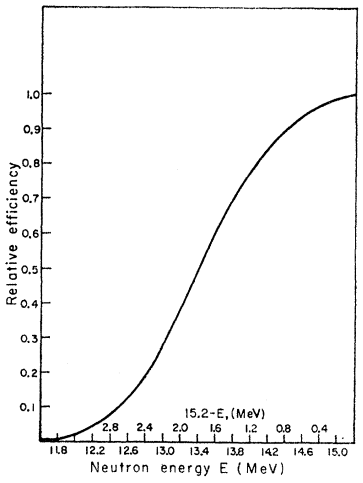

FIG. 3. Relative efficiency of detection of neutrons of energy E for "elastic peak" at 15.2 MeV.

as a function of laboratory scattering angle can be neglected for the heavy nuclei used as scatterers in this experiment),[9] and the counts in the same channels were summed and recorded as the "elastic counting rate" for the angle θ. In order to check the stability of the system, the detector was moved to zero degrees before and after each run at an angle θ, and the counts in the "elastic peak" recorded. The "zero normalized" counting rate, $C(\theta)$, is given by

$$C(\theta)=[C_{\text{in}}(\theta)-C_{\text{out}}(\theta)]/C_{\text{out}}(0), \tag{1}$$

where $C_{\text{in}}(\theta)$=number of counts per monitor count in the elastic scattering peak with the scatterer in the beam and the neutron detector at an angle θ with respect to the incident beam, $C_{\text{out}}(\theta)$=same as $C_{\text{in}}(\theta)$ but with the scatterer removed, and $C_{\text{out}}(0)$=same as $C_{\text{out}}(\theta)$ but with the neutron detector at zero degrees.

D. Data Reduction

Before comparing the results with the theoretical predictions, it is necessary to correct the data for effects of finite scatterer size, such as multiple scattering and attenuation, and for effects of beam divergence and finite detector size. It is also necessary to correct for the inelastically scattered neutrons included in the "elastic" counting rate. The largest corrections required were for the effects of multiple scattering and attenuation. The errors due to beam divergence and finite detector size were of the order of the experimental (counting) errors, and were not corrected for. These effects are most important in the deep, narrow first minimum of the angular distributions, and were masked in this experiment by the effect of multiple scattering. Because of the heavy target nuclei, no center-of-mass corrections were necessary, and all data are presented in the laboratory system of coordinates.

It is assumed that the zero normalized counting rate, $C(\theta)$, can be expressed as

$$C(\theta)=C_1(\theta)+C_{\text{m}}(\theta)+C_{\text{ne}}(\theta), \tag{2}$$

where $C_1(\theta)$=counting rate at the angle θ due to neutrons elastically scattered once, $C_{\text{m}}(\theta)$=counting rate at the angle θ due to neutrons elastically scattered two or more times, and $C_{\text{ne}}(\theta)$=counting rate at the angle θ due to nonelastic scattered neutrons. All counting rates are "zero normalized," and it is assumed that multiply inelastically scattered neutrons are effectively discriminated against by the time-of-flight system and may thus be ignored.

Since the effects of finite detector size are to be neglected, $C(\theta)$ will be regarded as the zero-normalized counting rate observed by an infinitesimal detector of solid angle $\Delta\Omega$, located at the angle θ.

If a beam of neutrons in the positive y direction is assumed incident on a cylindrical scatterer centered at the origin of a Cartesian coordinate system, with the z axis coinciding with the axis of the cylinder, the counting rate due to singly scattered neutrons is

$$C_1(\theta)=K^2N_S\sigma(\theta)A(\theta), \tag{3}$$

where

$$K^2=[(r_1+r_2)/r_1r_2]^2,$$

N_S=number of nuclei in the scatterer, $\sigma(\theta)$=differential cross section, $A(\theta)$=attenuation factor, r_1=distance from the neutron source to the scatterer, and r_2=distance from the scatterer to the detector; thus

$$\sigma(\theta)=[1/A(\theta)][C_1(\theta)/K^2N_S]. \tag{4}$$

The attenuation factor $A(\theta)$ is given by

$$A(\theta)=\frac{1}{V}\int\int\int\left(\frac{r_1}{r_1+y}\right)^2 \times\exp\left[-\frac{(R_0^2-x^2)^{1/2}+y+L(\theta)}{\lambda}\right]dxdydz, \tag{5}$$

where V=volume of the cylinder, R_0=radius of the cylinder, λ=mean free path of 15.2-MeV neutrons in the scatterer, $L(\theta)$=length from the point (x,y,z) to the surface $x^2+y^2=R_0^2$, in the direction θ.

The $x-y$ plane is the scattering plane, and θ is measured from the positive y axis. The integration extends over the volume of the scatterer. The mean free paths were calculated using the following estimates of the total neutron cross section: Ta: 5.2 b, Bi: 5.44 b, Th: 6.0 b, and U: 5.95 b. (These values were obtained by extrapolating published cross-section data[10] to 15.2 MeV.)

The differential cross section may be written in terms

[9] For light nuclei, this correction makes the cross section at backward angles very sensitive to the energy efficiency of the neutron counter. Lack of precise knowledge of this efficiency could be responsible for the disagreement at back angles for Al between refs. 4 and 7.

[10] R. J. Howerton, University of California Radiation Laboratory Report UCRL-6351, 1958 (unpublished).

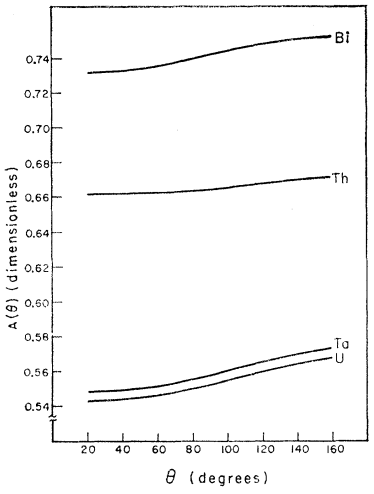

FIG. 4. Graph of attenuation factor $A(\theta)$ as a function of θ.

of the observed zero normalized counting rate as

$$\sigma(\theta)=\frac{1}{K^2N_sA(\theta)}\left[C(\theta)-C_m(\theta)-C_{ne}(\theta)\right]. \quad (6)$$

Monte Carlo methods were used to compute the probability per unit solid angle of a neutron scattering n times ($n\leq 4$) into an infinitesimal detector at various angles θ, in the scattering plane. The computation was done using neutron weights and forcing collisions in the scatterer. At each collision, a weight fraction σ_e/σ_t was chosen to undergo an elastic collision, and the scattering angle was determined from the differential cross section. $C_m(\theta)$ is proportional, in first order, to $(\sigma_e/\sigma_t)^2$, where σ_e is the total elastic cross section, and σ_t is the total cross section. The first approximation to σ_e is obtained by integrating Eq. (6) over all space, with $C_m(\theta)=C_{ne}(\theta)=0$. $C_m(\theta)$ is computed with this value of σ_e, and an iterative process is used to determine $\sigma(\theta)$ from Eq. (6), under the assumption that $C_{ne}(\theta)=0$.

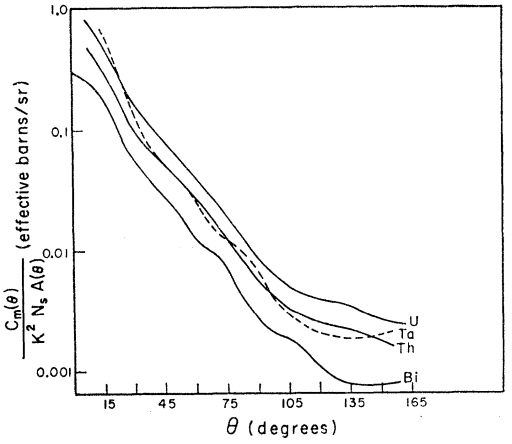

FIG. 5. Multiple scattering contribution to the measured cross section.

The attenuation factor $A(\theta)$ was evaluated by using an isotropic cross section for $\sigma(\theta)$ in the Monte Carlo computation and calculating only single scattering. Figure 4 shows $A(\theta)$ calculated for the four scatterers, and Fig. 5 shows the final results of the multiple scattering calculation.

$C_{ne}(\theta)$, the contribution to the observed "elastic" counting rate due to nonelastically scattered neutrons, is difficult to determine experimentally. A rough estimate was made by including additional channels in the "elastic scattering peak," and by assuming a constant level density in the energy region corresponding to the additional channels. This rough procedure indicated a contribution less than the statistical uncertainty at back angles. The situation is worse at forward angles due to the expected forward peaking of $C_{ne}(\theta)$. From the efficiency curve (Fig. 3), it is obvious that a large fraction of the neutrons inelastically scattered to the low-lying rotational levels of U and Th will be included in $C(\theta)$. The contributions from the higher single-particle states will be counted with less efficiency. Since a much better neutron energy resolution would be required to experimentally determine $C_{ne}(\theta)$, no attempt was made to correct the data for $C_{ne}(\theta)$. It is quite possible that $C_{ne}(\theta)$ has a noticeable effect at the first minimum, and this should be born in mind when comparing the results with theoretical predictions.

III. RESULTS AND CONCLUSIONS

The corrected data are presented in Figs. 6 through 9. The errors shown are probable errors, and include the effects of counting statistics and errors in the multiple scattering correction. There are additional uncertainties due to the finite size of the detector and due to beam divergence which could result in additional errors (of the order of the counting statistics) in the first minimum. Uncertainties in the geometric factors used in reducing the data could also introduce an absolute error estimated not to exceed 4%.

The solid lines represent the theoretical predictions of Bjorklund and Fernbach, using the following (spherical) optical potential:

$$V(r,E)=V_{cr}(E)\rho(r)+iV_{ci}(E)e^{-(r-R)^2/b^2}$$
$$+\frac{V_{sr}}{r}\frac{\hbar^2}{(\mu c)^2}\frac{\partial\rho(r)}{\partial r}\boldsymbol{\sigma}\cdot\mathbf{l},$$

TABLE I. Comparison of cross sections.

Element	$\sigma_t-\sigma_{ne}$ (b)	σ_e Bjorklund–Fernbach	σ_e Experimental
Ta	2.9 ±0.2	2.87	2.63±0.20
Bi	2.8 ±0.1	2.78	2.64±0.20
Th	3.35±0.3	2.72	3.13±0.25
U	3.1 ±0.3	2.71	3.21±0.24

where

$$\rho(r)=\left[1+\exp\left(\frac{r-R}{a}\right)\right]^{-1}$$

and the following values of the parameters were used:

$$V_{or}=44 \text{ MeV}, \qquad R=1.25A^{1/3} \text{ F},$$
$$V_{oi}=11 \text{ MeV}, \qquad V_{sr}=8.3 \text{ MeV},$$
$$a=0.65 \text{ F}, \qquad b=1.00 \text{ F}.$$

Total elastic cross sections were obtained by integrating the observed angular distributions. In Table I, the results are compared with the theoretical predictions of Bjorklund and Fernbach and also with values of $\sigma_t-\sigma_{ne}$ extrapolated to 15.2 MeV from measured values at lower energy.[10]

As seen in Figs. 6 through 9, there is evidence of damping of the oscillations in the backward angles for the deformed nuclei Ta, Th, and U, the experimental points being, in general, above the theoretical predictions. In contrast, the results for bismuth and other nondeformed nuclei[6] show a much better agreement with the theoretical predictions. The deviations observed for the deformed nuclei from the spherical optical potential at 15.2 MeV are similar, but not quite as pronounced, as the deviations observed at 7 MeV for Ta.[3] The counting of inelastically scattered neutrons (measured under the "elastic peak" due to the finite energy resolution) would also have the effect of raising and smoothing the cross sections in the backward direction, an effect which would influence closed-shell nuclei such as Bi least, because of the fewer low-lying energy levels.

The proper theoretical computations to compare the data with would have to include both the effect of the nuclear deformation on the spherical optical potential, and the contribution due to neutrons scattered from the low-lying rotational levels of the nucleus. To our knowledge, no such computations are available at this time.

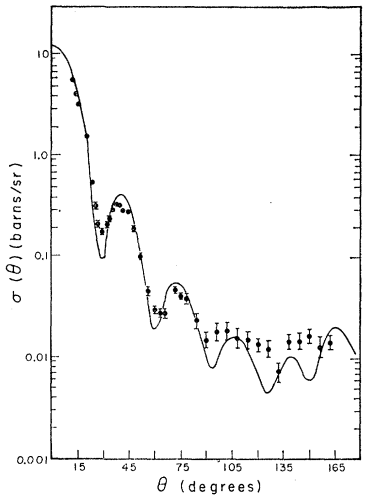

FIG. 6. Tantalum differential elastic cross section, 15.2-MeV neutron energy. The theoretical (solid) curve is from Bjorklund and Fernbach.

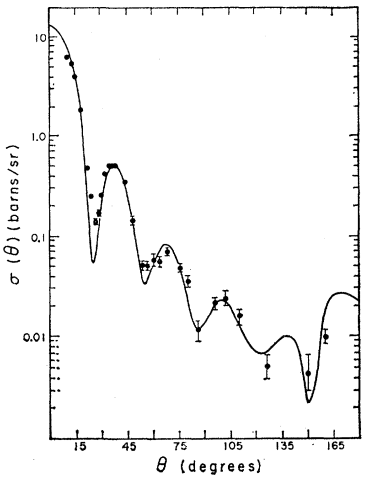

FIG. 7. Bismuth differential elastic cross section, 15.2-MeV neutron energy. The theoretical (solid) curve is from Bjorklund and Fernbach.

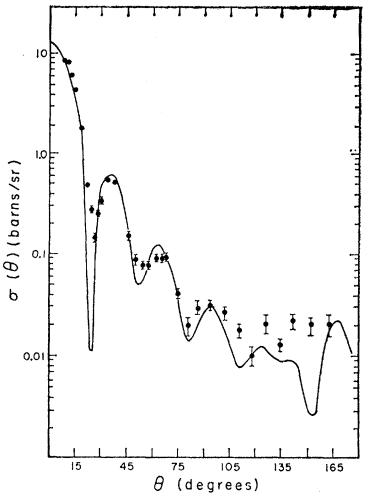

FIG. 8. Thorim differential elastic cross section, 15.2-MeV neutron energy. The theoretical (solid) curve is from Bjorklund and Fernbach.

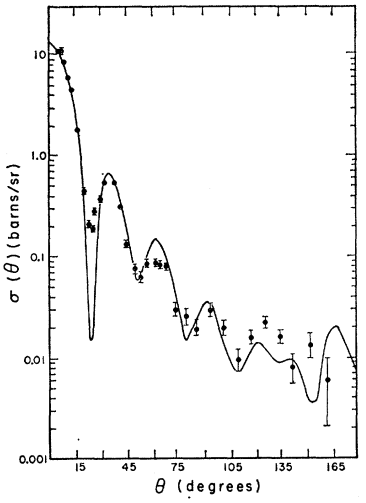

FIG. 9. Uranium differential elastic cross section, 15.2-MeV neutron energy. The theoretical (solid) curve is from Bjorklund and Fernbach.

It would, of course, be preferable to separate these "almost elastically" scattered neutrons experimentally. This could perhaps be done by (n',γ) coincidences. Such an experiment would require higher neutron fluxes than those which can be used with an associated particle time-of-flight system (which is limited by the counting rate in the alpha counter), and would present probelms in measuring low-energy gamma rays in a background of 14-MeV neutrons and higher energy gammas. A pulsed beam time-of-flight system could produce higher fluxes and alleviate the background problem somewhat, but would lack the inherent "collimation" of the associated particle technique.

ACKNOWLEDGMENTS

The Monte Carlo calculations were performed on the Burroughs 205 computer of the University of Virginia Computer Center. The authors wish to thank Dr. A. P. Batson and the staff of the computer center for their advice, and the University of Virginia for providing computer time for the calculation. We are grateful to the late Dr. Frank Bjorklund for having sent us the theoretical calculations for 15.2-MeV neutrons.

PHYSICAL REVIEW VOLUME 128, NUMBER 3 NOVEMBER 1, 1962

Cross Sections for Charged Particle Reactions Induced in Medium Weight Nuclei by Neutrons in the Energy Range 12–18 MeV†

F. GABBARD AND B. D. KERN
University of Kentucky, Lexington, Kentucky
(Received May 9, 1962)

Data are presented for (n,p) cross sections in Mg^{24}, Al^{27}, Ti^{48}, and Zn^{64}; and (n,α) reactions in Al^{27}, P^{31}, Mn^{55}, and Co^{59}. The neutron energy range was from 12 to 18 MeV. The experimental results are compared with statistical model calculations using an energy dependence of the level density of the form $\exp[2(aE^*)^{1/2}]$. Results of this comparison show that with the proper choice of the level-density and pairing-energy parameters the statistical model theory gives total (n,p) and (n,α) cross-section values in fair agreement with the experimental data. However, some of the parameters show marked deviations from expected trends.

I. INTRODUCTION

THE major impetus for measuring reaction cross sections in the medium and heavy elements is that such measurements are capable of yielding information about mechanisms by which the interaction between the incident nucleon and target nucleus proceeds. Recently there have been many measurements of total cross sections, angular distributions, and energy spectra of the reaction products produced in intermediate and heavy nuclei by incident particles of intermediate energy. In cases where final states are unresolved, the experimental results have been interpreted in terms of the statistical model of Weisskopf and Ewing.[1,2] This model has been only partially successful in explaining results of observations. The application of the statistical model has been reviewed by Le Couteur,[3] Peaslee,[4] and Gugelot.[5] Recent work on the application of the statistical model, particularly to (p,α) and (p,p') reactions, has been reviewed and extended by Sherr and Brady.[6] That the statistical model correctly explains many of the observed results is now generally accepted. However, there are many details still to be worked out.

The most sensitive way to check the predictions of the model is to compare calculated and measured energy spectra and angular distributions. If the model is to be applicable in a given reaction, the energy spectra must be "evaporation like" and the angular distributions must be nearly isotropic. In cases where applicability of the statistical assumptions is indicated, the energy spectra can be used to study the consistency of the assumed level density function and calculated compound nucleus formation cross sections.

Total reaction cross-section calculations are less model dependent since they lack information about spatial distribution; however, they can still provide useful information about the reaction mechanism. The results of such calculations must be consistent with observations for any acceptable model.

In the present report, total cross-section data on (n,p) and (n,α) reactions for elements varying in A from 24 to 64 are compared with statistical model calculations. The details of the experimental work are given in Sec. II and the formalism for the calculation of the reaction cross sections is discussed briefly in Sec. III.

† Partially supported by the U. S. Atomic Energy Commission.
[1] V. F. Weisskopf and D. H. Ewing, Phys. Rev. **57**, 472 (1940).
[2] J. M. Blatt and V. F. Weisskopf, *Theoretical Nuclear Physics* (John Wiley & Sons, Inc., New York, 1952), p. 340.
[3] K. J. LeCouteur, *Nuclear Reactions* (North-Holland Publishing Company, Amsterdam, 1959), Vol. 1, p. 318.
[4] D. C. Peaslee, Ann. Rev. Nuclear Sci. **5**, 99 (1955).
[5] P. D. Gugelot, reference 3, p. 39.
[6] R. Sherr and F. P. Brady, Phys. Rev. **124**, 1928 (1961).